Light- and pH-regulated Water-soluble Pseudorotaxanes Comprising a Cucurbit[7]uril and a Flavylium-based Axle

André Seco,[a] Shilin Yu,[b] Arnaud Tron,[b] Nathan D. McClenaghan,[b],* Fernando Pina,[a] A. Jorge Parola[a],* and Nuno Basílio[a],*

[a] André Seco, Prof. Fernando Pina, Prof. A. Jorge Parola, Dr. Nuno Basílio

LAQV – REQUIMTE, Department of Chemistry, NOVA School of Science and Technology, FCT-NOVA, NOVA University of Lisbon, 2829-516 Caparica, Portugal

Email: ajp@fct.unl.pt,

Email: nuno.basilio@fct.unl.pt

[b] Dr. Shilin Yu, Dr. Arnaud Tron, Dr. Nathan D. McClenaghan

Institut des Sciences Moléculaires, CNRS UMR 5255, Univ. Bordeaux, 33405 Talence, France

Email: nathan.mcclenaghan@u-bordeaux.fr

Dedicated to Professor Vincenzo Balzani on the occasion of his 85th birthday.

Abstract

A linear double pyridinium-terminated thread comprising a central chalcone moiety is shown to provide two independent binding sites with similar affinity for cucurbit[7]uril (CB7) macrocycles in water as judged from NMR, UV-Visible and fluorescence spectroscopies. Association results in [2] and [3]pseudorotaxanes, which are both pH and photosensitive. Switching from the neutral chalcone to the cationic flavylium form upon irradiation at 365 nm under acidic conditions provided an enhanced CB7 association ($K_{1:1}$ increases from 1.2×10^5 M^{-1} to 1.5×10^8 M^{-1}), limiting spontaneous on-thread

cucurbituril shuttling. This co-conformational change in the [2]pseudorotaxane is reversible in the dark with $k_{obs} = 4.1 \times 10^{-4}$ s^{-1}. Threading the flavylium moiety into CB7 leads to a dramatic increase in the fluorescence quantum yield, from 0.29 in the free axle to 0.97 in the [2]pseudorotaxane and 1.0 in the [3]pseudorotaxane.

Introduction

Rotaxanes and pseudorotaxanes are archetypal examples of artificial molecular machines in which a linear molecule (axle) is threaded in a macrocycle (ring).[1,2] These (supra)molecular assemblies provide versatile platforms to investigate the relative molecular movement of their sub-components in response to external stimuli, often exhibiting biased Brownian motion.[3–12] Common types of stochastic molecular motion observed in these systems include shuttling of the ring between two or more recognition motifs (stations) present in the axle molecule and, in the case of pseudorotaxanes, threading-dethreading processes. Such simple stimuli-responsive topology changes are not only of high fundamental interest but are also often associated to the functional aspects of these systems. Some of the potential applications of (pseudo)rotaxanes that explore the controlled motion of their subcomponents include switchable catalysts, nanovalves for controlled drug-release, molecular transport, molecular muscles and molecular assemblers.[13,14,23,15–22]

Despite being less common, water-soluble (pseudo)rotaxanes offer the possibility to explore these systems for biological/biocompatible applications and investigate their operation in the same solvent where biological machines exert their function. In this context, cucurbit[n]urils (CBns) macrocycles have demonstrated great potential as building blocks for the construction of stimuli-responsive water-soluble

(pseudo)rotaxanes.[24–27] Structurally, CBns are highly symmetrical, rigid barrel-shaped macrocycles featuring a hydrophobic cavity and electronegative carbonyl-lined portals that confer unmatched binding affinities and outstanding selectivity towards complementary guest molecules.[28–32] In general, the affinity of CBn macrocycles tends to increase for positively charged guests due to the formation of additional ion-dipole interactions between the carbonyl oxygen atoms and the guest's cationic groups.[33–36] These binding properties provide straightforward means to develop stimuli-responsive (pseudo)rotaxanes using pH or redox stimuli to control the ionization degree of the guest recognition sites.[26,37–41] Although the choice of light as a stimulus presents recognized advantages, such as remote application and high spatiotemporal control, light-responsive CBn-based (pseudo)rotaxanes, and host-guest complexes in general, have been less frequently reported.[42–56] This is likely due to the fact that the outcome of photoinduced conformational changes, observed in typical photochromic compounds, on the stability of the CBn-based host-guest systems is more difficult to predict.

Flavylium-based photoswitches, which typically interconvert between a neutral *trans*-chalcone and a positively charged flavylium cation, offer very interesting characteristics to be harnessed as photoresponsive components in the construction of artificial molecular machines[44,54,57–64] In this work we report the formation and detailed characterization of a water-soluble photoresponsive/fluorescent pseudorotaxane formed from a flavylium-based axle and cucurbit[7]uril (CB7) macrocycle (Scheme 1). We show that the molecular shuttling motion of CB7 along the axle can be efficiently controlled by light and pH stimuli. The emission of the chosen flavylium moiety was enhanced in the assembly allowing monitoring of the pseudorotaxane operation by fluorescence spectroscopy.

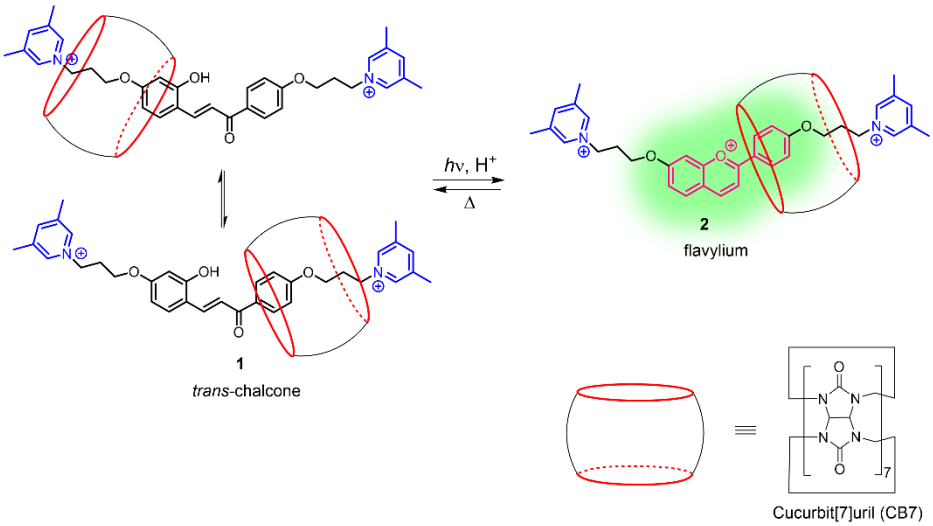

Scheme 1 – Photoresponsive water-soluble pseudorotaxanes based on a *trans*-chalcone/flavylium photoswitch with fluorescence reporting output.

Results and Discussion

The target dicationic *trans*-chalcone-based molecular axle **1** was synthesized according to the strategy presented in Scheme 2. Condensation of the easily prepared salicylaldehyde[65] (**3**) and acetophenone[44] (**4**) precursors, decorated with bromopropyl pendant groups, in acidic conditions leads to the formation of the flavylium cation (**5**). Hydrolysis of this species in neutral methanol:water solution gives the corresponding *trans*-chalcone (**6**). After extraction with dichloromethane, this compound was treated with 3,5-lutidine in acetonitrile to yield the target *trans*-chalcone **1**.

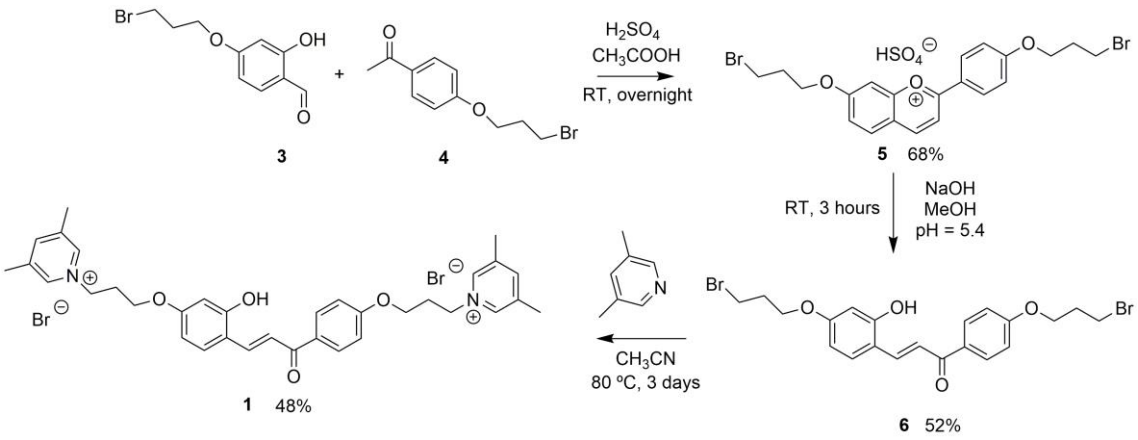

Scheme 2 – Adopted synthetic strategy to obtain **1**.

The formation of host-guest complexes between *trans*-chalcone **1** and CB7 was firstly investigated by UV-Vis absorption spectroscopy at pH ≈ 6.3 (in the absence of buffers). Guest **1** comprises two pyridinium binding sites for CB7 which can be anticipated to display similar (microscopic) binding affinity for this macrocyclic receptor, leading to the sequential formation of 1:1 and 2:1 host:guest complexes, as illustrated in Scheme 3.

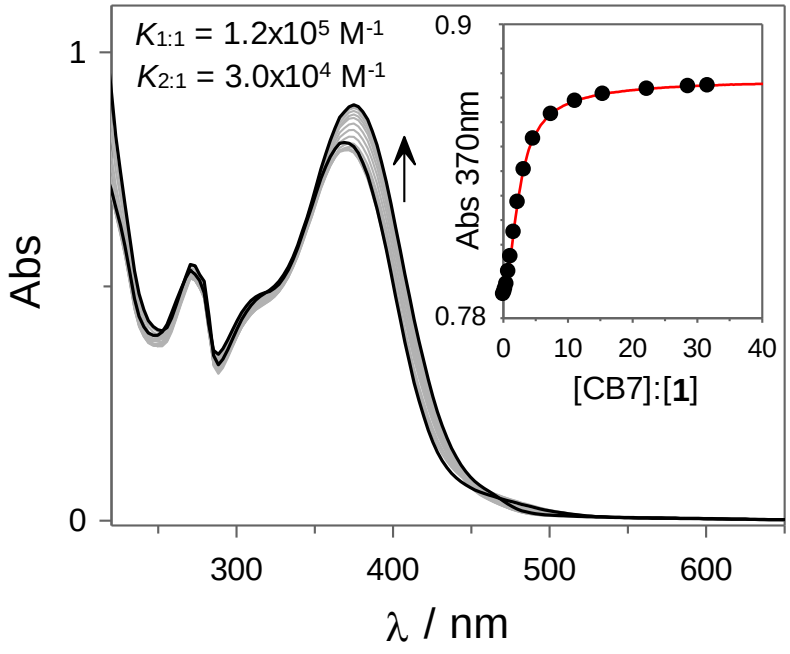

Figure 1 – UV-Vis absorption spectra of *trans*-chalcone **1** (30 μM) in the presence of increasing concentrations of CB7 in water (pH ≈ 6.3). Inset: Absorbance at 370 nm on adding increasing amounts of CB7.

The UV-Vis titration data of Figure 1 can be satisfactorily fit to a statistical 2:1 host:guest complexation model, i.e. assuming, as an approximation, that the formation of 2:1 complexes is non-cooperative and involves independent binding events ($K_{2:1} = K_{1:1}/4$), to retrieve the following binding constants: $K_{1:1} = 1.2 \times 10^5$ M^{-1} and $K_{2:1} = 3.0 \times 10^4$ M^{-1}.[66] It is worth noting that this model also implies that in the 1:1 complex, the CB7 wheel is statistically distributed between the two pyridinium binding sites of **1** leading to [2]pseudorotaxanes with two different co-conformations. This mechanistic proposal is supported by the well-known recognition properties of CB7 towards organic cations[28,67,68] and by ^{1}H NMR titration experiments (Figure 2) showing considerable signal broadening most likely due to an intermediate exchange regime in the chemical shift time scale between free **1** and CB7 and the two co-conformers of the 1:1 and the 2:1 host-guest species. It is noteworthy that for concentrations up to 1 equiv. of CB7 with respect to **1**, the ^{1}H NMR signals a,a', b,b' and c,c' assigned to the protons of the pyridinium units seems to be less affected than the remaining signals, indicating that these moieties remain mostly outside the cavity of CB7 (see 1:1 complex in Scheme 3). At higher concentrations, this observation holds only for signals assigned to protons a,a', suggesting that in the 2:1 complex the pyridinium units are partially encapsulated.

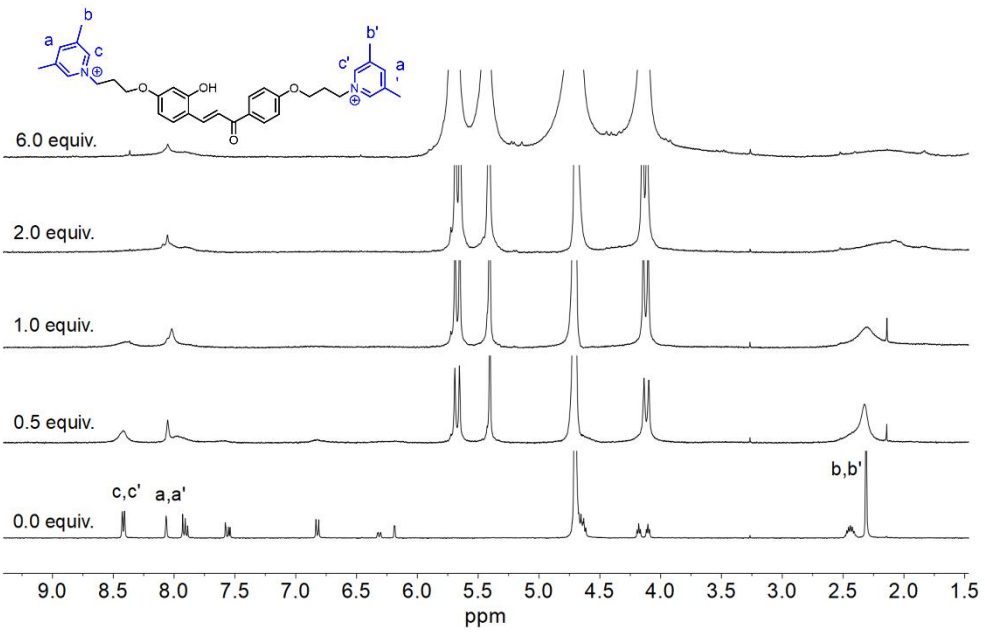

Figure 2 – ^{1}H NMR spectra of **1** (0.5 mM) in the presence of increasing concentrations of CB7 in D_2O. Upon addition of CB7, the ^{1}H NMR signals of **1** show considerable broadening likely due to intermediate exchange between free and complexed species with different co-conformations and stoichiometries.

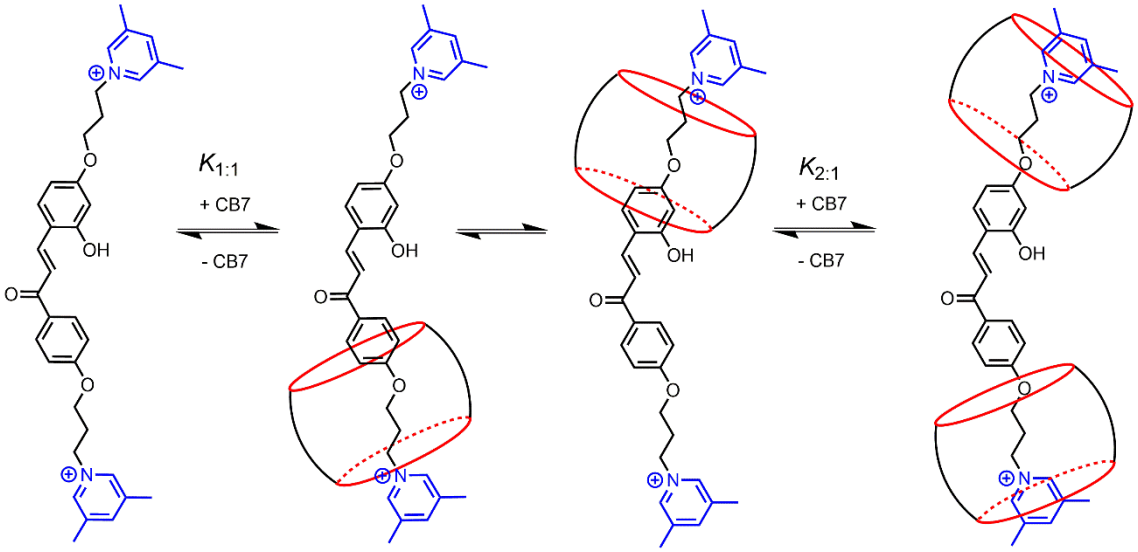

Scheme 3 – Proposed mechanism for the sequential formation of 1:1 and 2:1 host-guest complexes between *trans*-chalcone **1** and CB7.

Having demonstrated the formation of [2] and [3]pseudorotaxane host-guest complexes between *trans*-chalcone **1** and CB7, we turn our attention to the flavylium species **2**, that can be quantitatively obtained upon irradiation of *trans*-chalcone **1** at acidic pH values (see Supporting Information). Figure 3a shows the UV-Vis absorption spectra of **2** in the presence of increasing concentration of CB7 at pH = 1. Despite the small variations observed during the host-guest titrations, the observed biphasic trend (see inset in Figure 3a) is compatible with the formation of 1:1 and 2:1 host:guest complexes. These data can be satisfactorily fit to a sequential 2:1 host:guest binding model, allowing the determination of the lower limit of $K_{1:1} > 1 \times 10^7$ M^{-1} and a value for $K_{2:1} = 2.4 \times 10^4$ M^{-1}. Because the high value of $K_{1:1}$ prevents its accurate calculation from UV-Vis data, we proceeded to its determination in more dilute conditions using fluorescence spectroscopy. As can be observed from Figure 3b, the formation of host-guest complexes between flavylium **2** and CB7 leads to an increase in the luminescence intensity, which is more significant for the concentration range corresponding to the formation of the 1:1 complex. Using the fluorescence quantum yield of flavylium **2**, which was determined to be $\Phi_{em} = 0.29$ (in aqueous 0.1 M HCl solution) using acridine orange as a fluorescence standard (see Supporting Information), we plotted the apparent fluorescence quantum yield (Φ_{obs}) against the CB7 concentration (see inset of Figure 3b) and fitted these data to the previously mentioned 2:1 binding mode to retrieve the following binding constants: $K_{1:1} = 1.5 \times 10^8$ M^{-1} and $K_{2:1} = 2.4 \times 10^4$ M^{-1}. It should be noted that, while the UV-Vis titration allows the determination of $K_{2:1}$ with high accuracy, for the titration monitored by spectrofluorimetry it is the $K_{1:1}$ that can be determined with higher accuracy (see blue dotted line in the inset of Figure 3b for a fitting considering only a 1:1 model). A global fitting of the UV-Vis and fluorescence data in Figure 3 leads to $K_{1:1} = 1.5 \times 10^8$ M^{-1} and $K_{2:1} = 2.4 \times 10^4$ M^{-1}. The fact that $K_{1:1}$ is much higher than $K_{2:1}$ shows that in this case –

and differently from *trans*-chalcone **1** – the two pyridinium binding sites are not equivalent, as demonstrated below through ^{1}H NMR data. On the other hand, it should be noted that the $K_{2:1}$ value observed for the flavylium species **2** is close to the one observed for the *trans*-chalcone **1**, suggesting in both cases that the formation of the 2:1 complex corresponds to the complexation of CB7 with a pyridinium-centred binding site. Because the excitation wavelength was set at an isosbestic point, the data fit procedure also optimizes the fluorescence quantum yields for the [2]pseudorotaxanes (Φ_{em} = 0.97) and for the [3]pseudorotaxane (Φ_{em} = 1.0) in aqueous 0.1 M HCl solution.

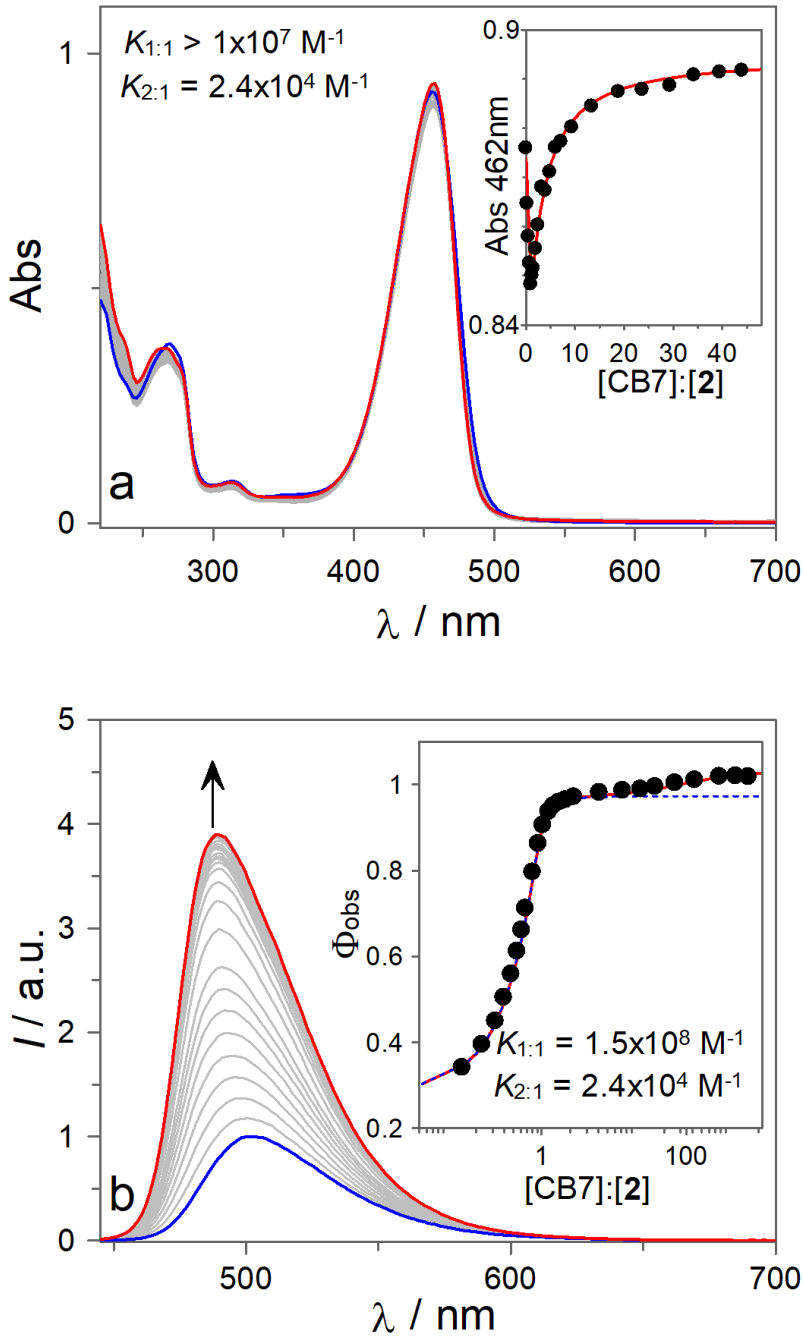

Figure 3 – (**a**) UV-Vis absorption spectra of flavylium **2** (15 μM) in the presence of increasing concentrations of CB7 in water at pH = 1. Inset: Absorbance at 462 nm on increasing amount of CB7; (**b**) Emission spectra of flavylium **2** (0.5 μM) in the presence of increasing concentrations of CB7 in water at pH = 1 (λ_{ex} = 430 nm, excitation slits = 9 nm, emission slits = 4.5 nm). Inset: observed fluorescence quantum yield on increasing

amount of CB7. Traced blue line is the fitting to a 1:1 model ($K_{1:1}$ = 1.5 × 10^8 M^{-1}) and the red line to a sequential 2:1 model.

The formation of pseudorotaxanes between flavylium **2** and CB7 was also demonstrated by ^{1}H NMR. In contrast to **1**, the addition of 0.5 equiv. of CB7 to a D_2O solution of **2** at pD = 1 leads to the appearance of a new set of signals, in slow exchange with those of free **2** that can be assigned to the presence of [2]pseudorotaxanes (see Figure 4). After addition of 1 equivalent of CB7 the signals of free **2** completely vanish and only the signals of the [2]pseudorotaxanes are observed, in agreement with the high binding constant for the formation of the 1:1 complex (99.8% association at the NMR concentrations in Figure 4). From the complexation-induced chemical shifts (CIS) pattern, it can be straightforwardly proposed that the region comprising the upfield shifted protons l, m and f' is deeply included in the CB7 cavity while c' and b' protons of the pyridinium unit are shifted downfield indicating that this region is located near the carbonyl portal of the receptor (see Scheme 4 for the proposed structure). Upon addition of CB7 concentrations above 1 equivalent, further changes are observed in the NMR spectra supporting the formation of 2:1 host-guest complexes ([3]pseudorotaxanes). Analysis of the spectrum acquired with 5 equiv. of CB7 (corresponding to 98% of 2:1 complex according to the reported binding constants and the NMR concentrations in Figure 4) shows that the signals corresponding to the pyridinium protons a, b and c undergo upfield shifts while the signals of protons g and h shift downfield (relative to the 1:1 complex). This pattern clearly suggests that the second CB7 ring binds to the pyridinium group appended to the pyrylium moiety (see proposed structure in Scheme 4) without affecting the position of the first CB7 receptor (please note that signals of protons m, l, a', b', c', d', e', f' remain practically unaffected when going from the 1:1 to the 2:1

complex). This feature suggests that both CB7 molecules are distant enough to avoid repulsive interactions between their carbonyl-lined portals (a feature that supports the statistical binding suggested for *trans*-chalcone **1** above, i.e., the two pyridinium sites bind with similar microscopic *K*).

The formation of the [2]pseudorotaxanes and [3]pseudorotaxanes was also supported by DOSY NMR experiments (see SI). Apparent diffusion coefficients of D_{obs} = 3.2 × 10^{-10} m^2 s^{-1}, 2.2 × 10^{-10} m^2 s^{-1} and 1.9 × 10^{-10} m^2 s^{-1} were determined in D_2O ([DCl] = 0.1 M) for the free flavylium **2**, the 1:1 complex (1 equiv. of CB7) and the 2:1 complex (5 equiv. of CB7), respectively. The decreasing trend in D_{obs} is in line with the sequential formation of larger molecular weight assemblies with increasing CB7:**1** mole ratio, as expected for the proposed binding model.

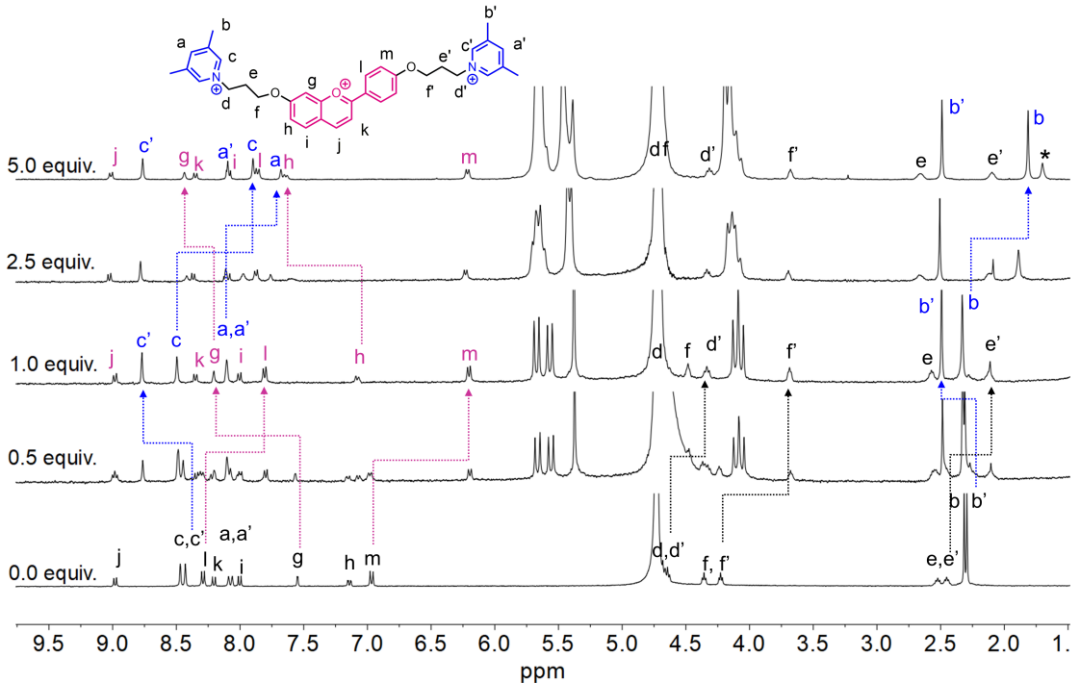

Figure 4 – ^{1}H NMR spectra of **2** (1.5 mM) in the presence of increasing concentrations of CB7 in D_2O at pD = 1 ([DCl] = 0.1 M). Contrary to **1**, in this case the slow exchange between free and complexed species with defined stoichiometry and co-conformation

leads to the observation of sharper signals in the ^{1}H NMR spectra. * denotes a minor impurity.

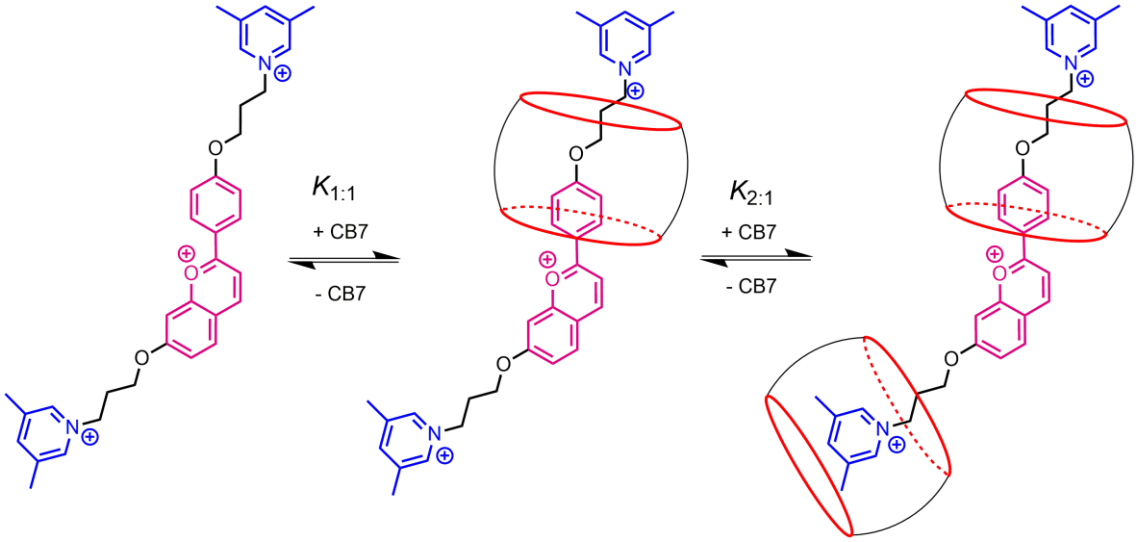

Scheme 4 – Proposed mechanism for the sequential formation of 1:1 and 2:1 host-guest complexes between flavylium **2** and CB7.

With the pseudorotaxanes fully characterized in terms of the binding affinity, stoichiometry and structure of the pseudorotaxanes, we focused on stimuli-responsive interconversion between *trans*-chalcone- and flavylium-based [2]pseudorotaxanes. Similarly to other 2-hydroxychalcone derivatives, *trans*-chalcone **1** can be reversibly converted into flavylium **2** either under strongly acidic conditions or by photochemical irradiation at slightly acidic pH values.

For free **1**, an apparent pK'_a = 1.8 was observed (see Supporting Information) for the *trans*-chalcone/flavylium thermal acid-base interconversion. It must be noted that the conversion of **1** (λ_{max} = 370 nm) into the respective yellow colored flavylium cation **2** (λ_{max} = 456 nm) is controlled by the thermal *trans*-cis isomerization of the chalcone,

taking several hours to achieve the equilibrium at the most acidic pH values. A similar behavior can be observed in the presence of 1 equivalent of CB7, for the [2]pseudorotaxanes, but in this case a pK'_a = 4.5 was observed. This large upward shift of $\Delta pK'_a$ = 2.8 upon binding reflects the fact that the flavylium species binds approximately 1000-fold more strongly to CB7 (Figure 5) than its respective *trans*-chalcone. Although there are some exceptions, upward pK_a shifts are typically observed for the CBn host-guest complexes due to their generally higher selectivity for acid species relative to their conjugate bases.[33–36]

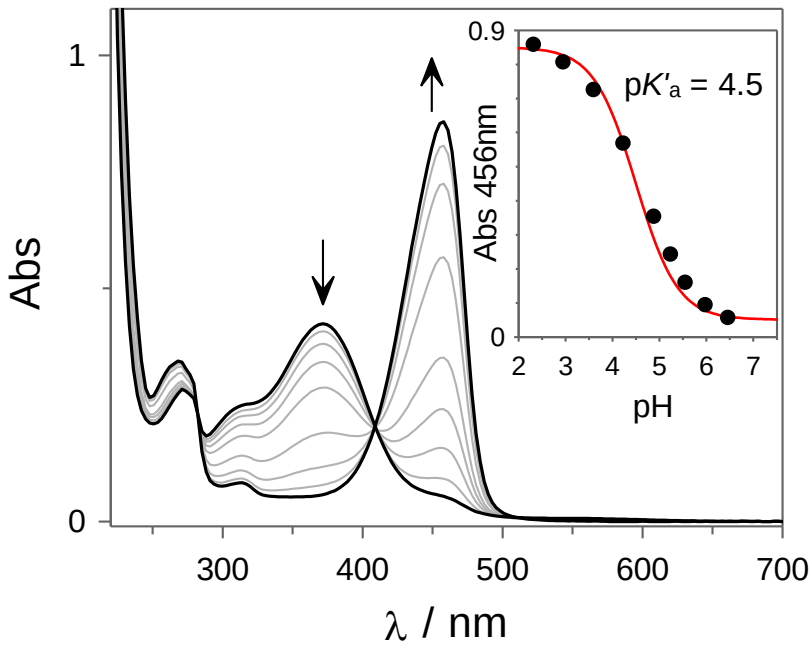

Figure 5 – UV-Vis absorption spectra of equilibrated solutions of **1** (18 μM) in the presence of 1 equivalent of CB7 in 10 mM of aqueous citrate buffer at different pH values. Inset: Absorbance at 456 nm as a function of pH.

Besides responding to a pH stimulus, chalcone-based (supra)molecular switches also respond to light. Upon irradiation, the *trans*-chalcone may undergo a *trans*-*cis* photoisomerization that yields the *cis*-chalcone. Once formed, this species may thermally revert to the *trans* isomer or further evolve to the flavylium cation through the formation of a hemiketal species with subsequent dehydration.[69] This last step is thermodynamically and kinetically favored in acidic conditions and therefore the photoinduced formation of the flavylium cation is more efficient under slightly acidic conditions. Figure 6 reports the spectral changes observed upon irradiation of the *trans*-chalcone **1** with 365 nm light, in the presence of 1 equiv. of CB7, at pH = 5.4. The *trans*-chalcone absorption band centered at 373 nm decreases to give rise to a new band centered at 457 nm, assigned to the flavylium species. From the absorption spectrum at the photostationary state it is possible to estimate that 85% of the *trans*-chalcone was converted into the flavylium-based [2]pseudorotaxane with a photochemical quantum yield of Φ_{photo} = 0.13. The system can be reverted to the *trans*-chalcone species in the dark with an observed rate constant of $k_{obs} = 4.1 \times 10^{-4}$ s^{-1} at 20 ºC.

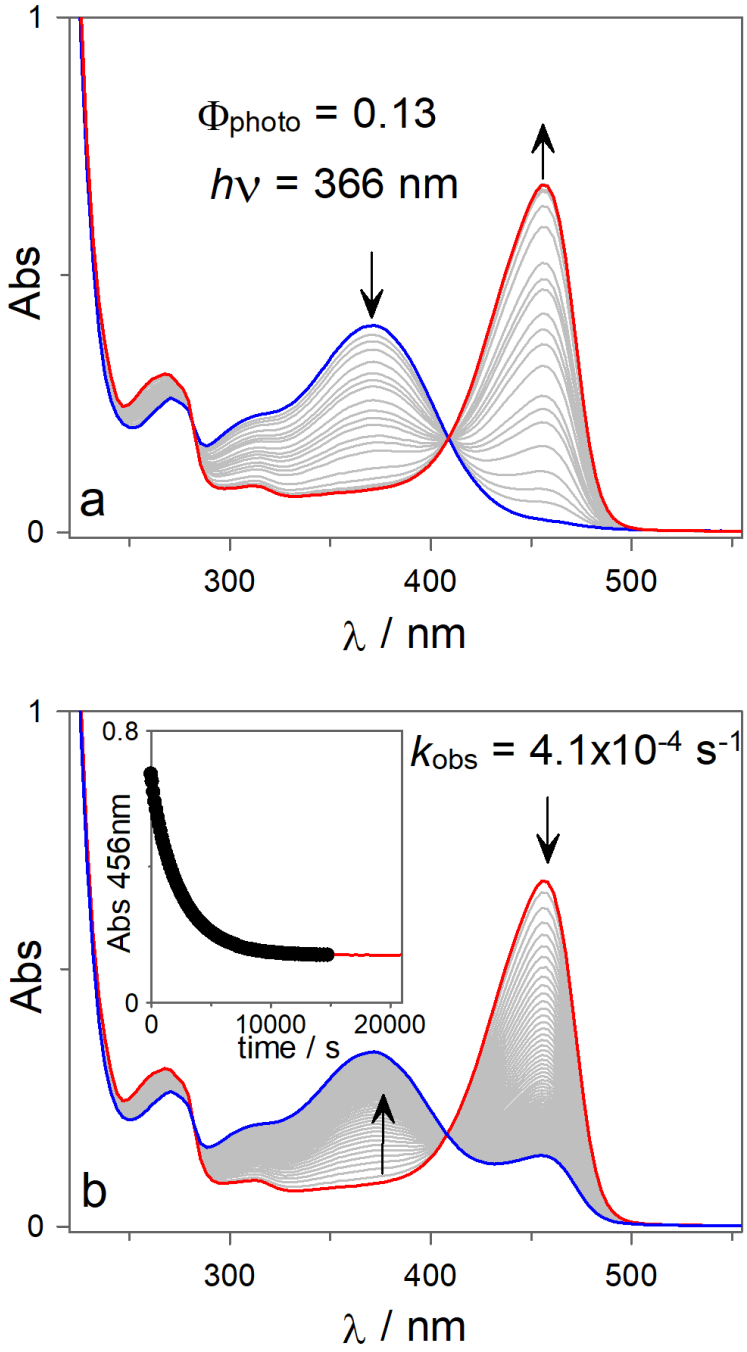

Figure 6 –(a) UV-Vis absorption spectra observed upon irradiation (365 nm) of an aqueous solution of **1** (18 μM) in the presence of 1 equiv. of CB7 at pH = 5.4 (10 mM of citrate buffer). (b) Thermal recovery from the photostationary state at 20 ºC.

It must be noted that, under these conditions, while the *trans*-chalcone **1** is present as a mixture of free thread, [2]pseudorotaxane and [3]pseudorotaxane species, flavylium **2** is present quasi-exclusively as a [2]pseudorotaxane owing to its very high stability constant ($K_{1:1} = 1.5 \times 10^8\ M^{-1}$). This system can thus be explored as a supramolecular switch where the threading/dethreading processes can be photochemically controlled in very dilute conditions (Scheme 5). For example, for equimolar solutions at 0.5 μM the free *trans*-chalcone **1** can be estimated to be the main species (95%) while for flavylium **2**, under the same conditions, the [2]pseudorotaxane is the predominant species (89%). On the other hand, at millimolar concentrations (0.5 mM) the main *trans*-chalcone **1** species are the [2]pseudorotaxanes (50%) that coexist with the free thread (27%) and [3]pseudorotaxane (23%) species. Thus, focusing on the [2]pseudorotaxane, light can be used to control the co-conformational behavior of this form, with CB7 distributed between the two pyridinium binding sites, that upon formation of the flavylium species binds predominantly to a single site as demonstrated by ^{1}H NMR experiments. Figure 7 shows the ^{1}H NMR spectra of *trans*-chalcone **1** in the presence of 1 equiv. of CB7 at pD = 1, featuring very broad signal due to the mixture of several species in intermediate exchange. Upon direct irradiation with 365 nm light, the *trans*-chalcone species are quantitatively converted into the flavylium [2]pseudorotaxane as can be confirmed from the single set of sharp signals assigned to this species.

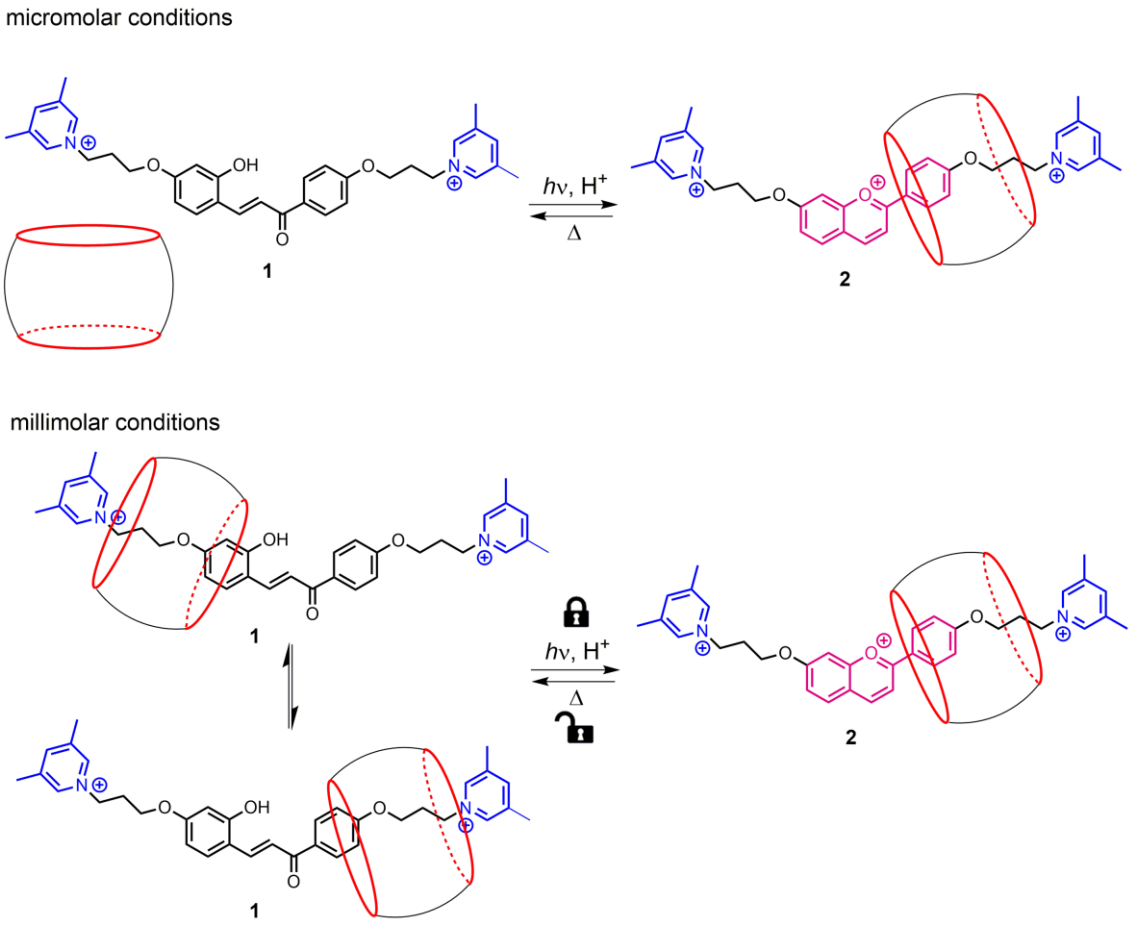

Scheme 5 – Concentration-dependent photoresponsive switching between threading/dethreading and co-conformational distribution in *trans*-chalcone-based [2]pseudorotaxanes. Note that under these conditions some free *trans*-chalcone thread and [3]pseudorotaxanes will be also present in solution.

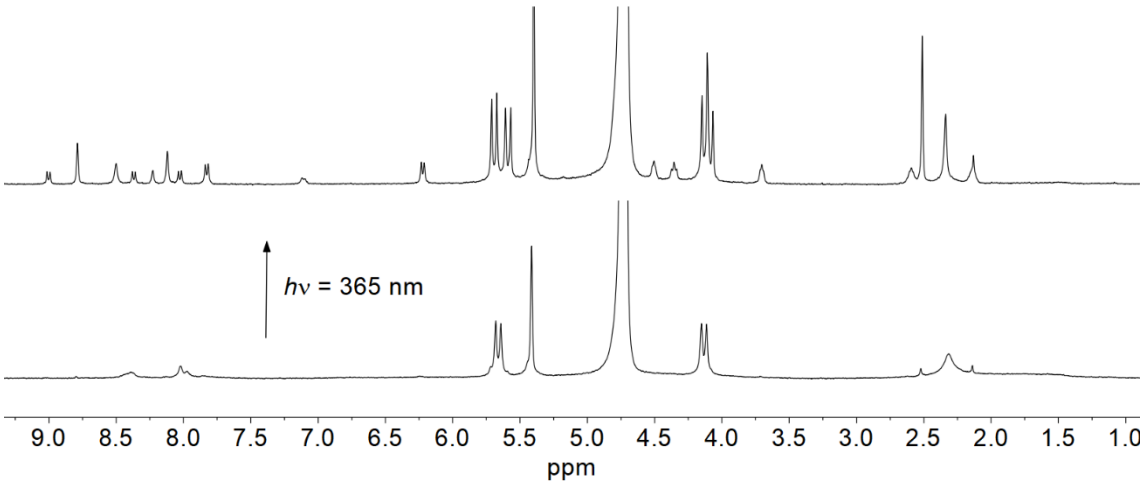

Figure 7 – ^{1}H NMR spectra of **1** (1.5 mM) in the presence 1 equiv. of CB7 in D_2O at pD = 1 ([DCl] = 0.1 M) before and after irradiation with 365 nm light (200 W Xe/Hg lamp, until full conversion).

The exceptional photochemical/photophysical properties of this system were also exploited to demonstrate the photoswitchable fluorescence properties of the pseudorotaxanes described herein. As can be observed from Figure 8, continuous irradiation of **1** at 365 nm, in the presence of 1 equiv. of CB7 at pH = 5, induces the photoisomerization of the *trans*-chalcone to form the flavylium cation-based pseudorotaxane and simultaneously excite this species (due to its residual absorption at this wavelength) allowing simultaneous monitoring of its formation by fluorescence detection. Switching the excitation wavelength to 480 nm, where the chalcone no longer absorbs, interrupts the energy supply that kept the system in an out-of-equilibrium dissipative state, and it starts to revert back to the initial *trans*-chalcone as can be observed from the first-order decay of the fluorescence signal. This process is reversible and can be repeated with minimal degradation.

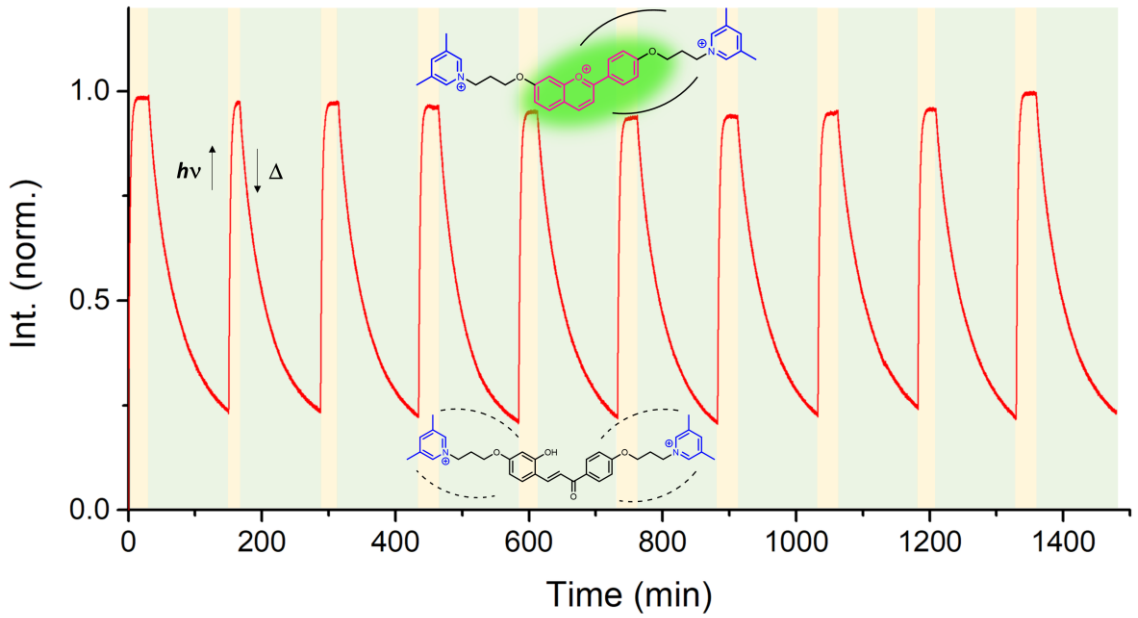

Figure 8 – Irradiation/recovery experiment. The yellow areas represent excitation at 365 nm and the green ones, excitation at 480 nm. This allows continuous excitation of the complexed flavylium cation but selective photo-induced isomerization of the *trans*-chalcone. The red trace represents the normalized flavylium emission read at 505 nm over 10 irradiation cycles (18 μM with 1 equivalent of CB7).

Conclusion

Herein we describe switchable water-soluble interpenetrating pseudorotaxane architectures. Threading a cucurbit[7]uril macrocycle with a linear double pyridinium-terminated thread comprising a central chalcone moiety is shown to give rise to a supramolecular architecture with two independent binding sites with similar affinity for cucurbit[7]uril (CB7) macrocycles in water as judged from NMR, UV-Visible and fluorescence spectroscopies, allowing for on-thread shuttling. The resulting pseudorotaxanes are shown to be both pH and photosensitive. Indeed, switching from the neutral chalcone to the cationic flavylium form upon irradiation under slightly acidic

conditions provided a station with circa 1000-fold enhanced CB7 association while the second station was minimally affected, limiting spontaneous on-thread cucurbituril shuttling. Interestingly, multicycle interconversion between the flavylium and chalcone forms, with accompanying regulation of cucurbituril motility, was shown to occur via fluorescence read-out, facilitated by the nearly unitary fluorescence quantum yield of the encapsulated flavylium moiety. Determining detailed information on dynamic architectures and their behaviour in response to stimuli in aqueous environments represent first steps towards interfacing biological media.

Experimental Section

Materials and Methods

Commercially available reagents were used without additional purification. NMR spectra were acquired using a Bruker Avance NEO operating at 500 MHz (^{1}H) or 125 MHz (^{13}C) or a Bruker Avance III operating at 400 MHz (^{1}H) or 101 MHz (^{13}C). DOSY experiments (^{1}H NMR diffusion) were made using the stimulated echo sequence using bipolar sine gradient pulses (ledbpgp2s). The pulsed gradients were applied with a linearly incremented power level, ranging from 1.59 to 46.2 G.cm^{-1}. The diffusion delay period (Δ) was set to 60 ms and for the encoding/decoding of the diffusion, 4 ms pulsed field gradients (δ) were used. The integral of some selected flavylium **2** ^{1}H NMR signals (typically b and/or b') was plotted against the gradient strength and that data was fitted with the Stejskal-Tanner equation to obtain the diffusion coefficient, D (see supporting information). Mass spectra were acquired on an Agilent 6200 series TOF/6500 series Q-TOF using flow injection analysis and electrospray ionization technique. Solutions were prepared in deionized water. The pH measurements were made using a Crison basic 20+

pH meter. Whenever necessary, 10 mM sodium citrate buffer was used with pH adjusted by addition of NaOH or HCl aqueous solutions. Spectroscopic experiments were performed with 1 cm quartz or plastic (Plastibrand®) cells using either a Cary100bio or 5000 spectrophotometer from Varian. A SPEX Fluorolog 1681 0.22m 150W Xe-Hg lamp was used for all fluorescence measurements and, when necessary, to irradiate solutions (without slits in excitation monochromator). Fluorescence quantum yields were determined using acridine orange in basic ethanol (Φ_{em} = 0.20) as fluorescence standard.[70] Photochemical quantum yields were calculated using ferrioxalate as actinometer.[71]

Synthesis

7-(3-Bromopropoxy)-2-(4-(3-bromopropoxy)phenyl)chromenylium hydrogen sulfate (flavylium **5**)

4'-Bromopropanoxyacetophenone[44] (**4**) was dissolved in 2 mL of acetic acid (200 mg, 0.77 mmol) and 198 mg (1.0 eq.) of 4-bromopropanoxysalicylaldehyde[65] (**3**) were added to the solution, followed by dropwise addition of conc. H_2SO_4 (300 µL). The mixture immediately started to change to a reddish color and was left overnight stirring at room temperature. When completed, the bulk product was precipitated in a 1:2 mixture (*v*/*v*) of diethyl ether and ethyl acetate. After filtration, the precipitate was thoroughly washed with diethyl ether and dried under vacuum. A red powder was obtained (253 mg, yield = 68%). ^{1}H NMR (500 MHz, MeOD) δ (ppm): 9.25 (d, J = 8.7 Hz, 1H), 8.61 (d, J = 9.0 Hz, 2H), 8.52 (d, J = 8.8 Hz, 1H), 8.26 (d, J = 9.0 Hz, 1H), 7.96 (s, 1H), 7.57 (dd, J = 9.0, 2.2 Hz, 1H), 7.35 (d, J = 8.9 Hz, 2H), 4.55 (t, J = 5.9 Hz, 2H), 4.39 (t, J = 5.9 Hz, 2H), 3.73 (t, J = 6.5 Hz, 2H), 3.69 (t, J = 6.5 Hz, 2H), 2.48 (p, J = 6.2 Hz, 2H), 2.41 (p, J = 6.2 Hz, 2H). ^{13}C NMR (126 MHz, MeOD) δ (ppm): 172.73, 168.33, 166.53, 159.10, 153.95,

132.68, 131.94, 121.50, 121.31, 119.66, 116.28, 113.50, 100.94, 67.94, 66.55, 31.76, 31.56, 28.98, 28.83. HRMS (ESI+) m/z calculated for $C_{21}H_{21}Br_2O_3^+$ [M^+]: 480.9831; found: 480.9832.

(E)-3-(4-(3-Bromopropoxy)-2-hydroxyphenyl)-1-(4-(3-bromopropoxy)phenyl)prop-2-en-1-one (*trans*-chalcone **6**)

Flavylium **5** (115 mg) was dissolved in methanol (30 mL) and aqueous 0.1M NaOH solution was slowly added until the solution reached pH = 5.40. The round bottom flask was then left sitting in the dark for 2 h, after which the solvent was removed under reduced pressure. The neutral chalcone was then extracted with the dichloromethane (three times, then brine) in order to remove the excess salts. The combined dichloromethane extracts were dried over sodium sulfate, the solvent was removed, and the product was dried under vacuum to yield a yellowish powder (52 mg, raw yield = 52%). The compound was used in the next step with no further purification. For analytical purposes, it can be further purified by column chromatography using 95:5 (v/v) dichloromethane: methanol. ^{1}H NMR (500 MHz, $CDCl_3$) δ (ppm): 8.17 (d, J = 15.7 Hz, 1H), 8.07 (d, J = 8.8 Hz, 2H), 7.62 (d, J = 15.7 Hz, 1H), 7.55 (d, J = 8.7 Hz, 1H), 7.00 (d, J = 8.8 Hz, 2H), 6.55 (dd, J = 8.7, 2.4 Hz, 1H), 6.50 (d, J = 2.4 Hz, 1H), 4.22 (t, J = 5.8 Hz, 2H), 4.14 (t, J = 5.8 Hz, 2H), 3.71 – 3.55 (m, 4H), 2.45 – 2.26 (m, 4H). ^{13}C NMR (126 MHz, $CDCl_3$) δ (ppm): 190.10, 162.40, 161.84, 157.48, 140.18, 131.62, 130.92, 130.60, 119.89, 115.79, 114.27, 107.81, 102.52, 65.53, 65.51, 32.18, 29.80, 29.74, 29.71. HRMS (ESI) m/z calculated for $C_{21}H_{22}Br_2NaO_4^+$ [M+Na^+]: 520.9757; found: 520.9756.

(E)-1-(3-(4-(3-(4-(3-(3,5-Dimethylpyridin-1-ium-1-yl)propoxy)-2-hydroxyphenyl)acryloyl)phenoxy)propyl)-3,5-dimethylpyridin-1-ium bromide (*trans*-Chalcone **1**)

Chalcone **6** (60 mg, 120 μmol) was dissolved in dry acetonitrile (3 mL). To this solution, 3,5-lutidine was added (140 μL, 10 eq.). The reaction was then left to stir at 80°C for 3 days, during which time a pale brown solid precipitated. After cooling to room temperature, the reaction mixture was kept at 4°C overnight, in a falcon tube. The following day the tube was centrifuged for 15 min (4500 rpm) with the precipitate forming a pale brownish pellet that was washed twice with acetonitrile. A loose powder was obtained and recrystallization from acetonitrile followed by a thorough wash with acetonitrile and diethyl ether yielded the final product as a pale yellow-green loose powder (32mg, yield = 48%) that was characterized by NMR: ^{1}H NMR (400 MHz, MeOD): δ (ppm): 8.65 (d, J = 5.3 Hz, 4H), 8.17 (s, 2H), 7.96 – 7.88 (m, 3H), 7.59 (d, J = 15.6 Hz, 1H), 7.51 (d, J = 8.7 Hz, 1H), 6.85 (d, J = 8.6 Hz, 2H), 6.29 (dd, J = 8.7, 2.4 Hz, 1H), 6.21 (d, J = 2.4 Hz, 1H), 4.69 (q, J = 6.9 Hz, 4H), 4.14 (t, J = 5.5 Hz, 2H), 4.06 (t, J = 5.5 Hz, 2H), 2.52 – 2.35 (m, 16H); ^{13}C NMR (101 MHz, CD_3OD): δ (ppm): 190.10, 162.03, 161.48, 159.09, 146.59, 146.54, 141.70, 140.51, 139.05, 139.00, 131.64, 130.69, 130.51, 118.64, 115.67, 113.97, 106.23, 101.20, 64.89, 64.74, 59.24, 59.12, 30.04, 16.87. HRMS (ESI) m/z calculated for $C_{35}H_{40}N_2O_4^{2+}$ [M^{2+}]: 276.1489; found: 276.1486.

Acknowledgements

This work was supported by the Associate Laboratory for Green Chemistry - LAQV which is financed by national funds from FCT/MCTES (UIDB/50006/2020). FCT/MCTES is also acknowledged for supporting the National Portuguese NMR

Network (ROTEIRO/0031/2013-PINFRA/22161/2016, cofinanced by FEDER through COMPETE 2020, POCI, PORL, and FCT through PIDDAC) and for grants PTDC/QUI-QFI/30951/2017 and 2020.07313.BD (AS). China Scholarship Council (SY) is acknowledged.

Keywords: Chalcones; Flavylium; Photochemistry; Rotaxanes; Supramolecular Chemistry

References

[1] V. Balzani, A. Credi, M. Venturi, *Molecular Devices and Machines– A Journey into the Nano World*, Wiley, Weinheim, **2003**.

[2] C. J. Bruns, J. F. Stoddart, *The Nature of the Mechanical Bond*, Wiley, Hoboken, **2016**.

[3] F. M. Raymo, J. F. Stoddart, M. Raymo, P. Incorporating, C. Ethers, *Chem. Rev.* **1999**, *99*, 1643–1664.

[4] V. Balzani, M. Gómes-López, J. F. Stoddart, *Acc. Chem. Res.* **1998**, *31*, 405–414.

[5] S. Erbas-Cakmak, D. A. Leigh, C. T. McTernan, A. L. Nussbaumer, *Chem. Rev.* **2015**, *115*, 10081–10206.

[6] S. Kassem, T. van Leeuwen, A. S. Lubbe, M. R. Wilson, B. L. Feringa, D. A. Leigh, *Chem. Soc. Rev.* **2017**, *46*, 2592–2621.

[7] A. Goswami, S. Saha, P. K. Biswas, M. Schmittel, *Chem. Rev.* **2020**, *120*, 125–199.

[8] M. Baroncini, S. Silvi, A. Credi, *Chem. Rev.* **2020**, *120*, 200–268.

[9] M. Xue, Y. Yang, X. Chi, X. Yan, F. Huang, *Chem. Rev.* **2015**, *115*, 7398–7501.

[10] R. Ballardini, V. Balzani, A. Credi, M. T. Gandolfi, M. Venturi, *Acc. Chem. Res.* **2001**, *34*, 445–455.

[11] V. Balzani, A. Credi, M. Venturi, *Chem. Soc. Rev.* **2009**, *38*, 1542.

[12] S. Yu, N. D. McClenaghan, J. L. Pozzo, *Photochem. Photobiol. Sci.* **2019**, *18*, 2102–2111.

[13] V. Blanco, D. A. Leigh, V. Marcos, *Chem. Soc. Rev.* **2015**, *44*, 5341–5370.

[14] W. Chen, C. A. Glackin, M. A. Horwitz, J. I. Zink, *Acc. Chem. Res.* **2019**, *52*, 1531–1542.

[15] E. Moulin, L. Faour, C. C. Carmona-Vargas, N. Giuseppone, *Adv. Mater.* **2020**, *32*, 1906036.

[16] N. Song, Y.-W. Yang, *Chem. Soc. Rev.* **2015**, *44*, 3474–3504.

[17] S. Chen, Y. Wang, T. Nie, C. Bao, C. Wang, T. Xu, Q. Lin, D.-H. Qu, X. Gong, Y. Yang, et al., *J. Am. Chem. Soc.* **2018**, *140*, 17992–17998.

[18] C. Schäfer, G. Ragazzon, B. Colasson, M. La Rosa, S. Silvi, A. Credi, *ChemistryOpen* **2016**, *5*, 120–124.

[19] C. Cheng, P. R. McGonigal, W. Liu, H. Li, N. A. Vermeulen, C. Ke, M. Frasconi, C. L. Stern, W. A. Goddard III, J. F. Stoddart, *J. Am. Chem. Soc.* **2014**, *136*, 14702–14705.

[20] J.-P. Collin, C. Dietrich-Buchecker, P. Gaviña, M. C. Jimenez-Molero, J.-P. Sauvage, *Acc. Chem. Res.* **2001**, *34*, 477–487.

[21] C. J. Bruns, J. F. Stoddart, *Acc. Chem. Res.* **2014**, *47*, 2186–2199.

[22] R. Herges, *Chem. Sci.* **2020**, *11*, 9048–9055.

[23] Y. Qiu, B. Song, C. Pezzato, D. Shen, W. Liu, L. Zhang, Y. Feng, Q.-H. Guo, K. Cai, W. Li, et al., *Science* **2020**, *368*, 1247–1253.

[24] L. Zhu, M. Zhu, Y. Zhao, *ChemPlusChem* **2017**, *82*, 30–41.

[25] N. Basílio, U. Pischel, in *Cucurbituril-Based Functional Materials*, The Royal Society Of Chemistry, **2019**, pp. 56–94.

[26] V. Sindelar, S. Silvi, S. E. Parker, D. Sobransingh, A. E. Kaifer, *Adv. Funct. Mater.* **2007**, *17*, 694–701.

[27] A. E. Kaifer, *Acc. Chem. Res.* **2014**, *47*, 2160–2167.

[28] S. J. Barrow, S. Kasera, M. J. Rowland, J. del Barrio, O. A. Scherman, *Chem. Rev.* **2015**, *115*, 12320–12406.

[29] K. I. Assaf, W. M. Nau, *Chem. Soc. Rev.* **2015**, *44*, 394–418.

[30] L. Isaacs, *Acc. Chem. Res.* **2014**, *47*, 2052–2062.

[31] D. Shetty, J. K. Khedkar, K. M. Park, K. Kim, *Chem. Soc. Rev.* **2015**, *44*, 8747–8761.

[32] E. Masson, X. Ling, R. Joseph, L. Kyeremeh-Mensah, X. Lu, *RSC Adv.* **2012**, *2*, 1213–1247.

[33] J. Mohanty, a C. Bhasikuttan, W. M. Nau, H. Pal, *J. Phys. Chem. B* **2006**, *110*, 5132–5138.

[34] A. I. Lazar, J. Rohacova, W. M. Nau, *J. Phys. Chem. B* **2017**, *121*, 11390–11398.

[35] N. Basílio, S. Gago, A. J. Parola, F. Pina, *ACS Omega* **2017**, *2*, 70–75.

[36] N. Basílio, J. Mendoza, S. Gago, A. J. Parola, *Chem. Commun.* **2017**, *53*, 6472–6475.

[37] A. E. Kaifer, W. Li, S. Silvi, V. Sindelar, *Chem. Commun.* **2012**, *48*, 6693–6695.

[38] D. Sobransingh, A. E. Kaifer, *Org. Lett.* **2006**, *8*, 3247–3250.

[39] V. Sindelar, S. Silvi, A. E. Kaifer, *Chem. Commun.* **2006**, 2185.

[40] S. Im Jun, J. Wook Lee, S. Sakamoto, K. Yamaguchi, K. Kim, *Tetrahedron Lett.* **2000**, *41*, 471–475.

[41] J. Wook Lee, K. Kim, K. Kim, *Chem. Commun.* **2001**, 1042–1043.

[42] E. Pazos, P. Novo, C. Peinador, A. E. Kaifer, M. D. García, *Angew. Chem. Int. Ed.* **2019**, *58*, 403–416. *Angew. Chem.* **2019**, *131*, 409– 422.

[43] J. Vázquez, M. A. Romero, R. N. Dsouza, U. Pischel, *Chem. Commun.* **2016**, *52*, 6245–6248.

[44] A. Zubillaga, P. Ferreira, A. J. Parola, S. Gago, N. Basílio, *Chem. Commun.* **2018**, *54*, 2743–2746.

[45] M. A. Romero, N. Basílio, A. J. Moro, M. Domingues, J. A. González-Delgado, J. F. Arteaga, U. Pischel, *Chem. - A Eur. J.* **2017**, *23*, 13105–13111.

[46] N. Basílio, U. Pischel, *Chem. - A Eur. J.* **2016**, *22*, 15208–15211.

[47] M. Colaço, P. Máximo, A. Jorge Parola, N. Basílio, *Chem. – A Eur. J.* **2021**, chem.202100974.

[48] R. J. Fernandes, P. Remón, A. J. Moro, A. Seco, A. S. D. Ferreira, U. Pischel, N. Basílio, *J. Org. Chem.* **2021**, *86*, 8472–8478.

[49] F. Tian, D. Jiao, F. Biedermann, O. A. Scherman, *Nat. Commun.* **2012**, *3*, 1207.

[50] J. del Barrio, S. T. J. Ryan, P. G. Jambrina, E. Rosta, O. A. Scherman, *J. Am. Chem. Soc.* **2016**, *138*, 5745–5748.

[51] J. del Barrio, P. N. Horton, D. Lairez, G. O. Lloyd, C. Toprakcioglu, O. A. Scherman, *J. Am. Chem. Soc.* **2013**, *135*, 11760–11763.

[52] E. Y. Chernikova, D. V. Berdnikova, Y. V. Fedorov, O. A. Fedorova, F. Maurel, G. Jonusauskas, *Phys. Chem. Chem. Phys.* **2017**, *19*, 25834–25839.

[53] Y. V. Fedorov, S. V. Tkachenko, E. Y. Chernikova, I. a. Godovikov, O. a. Fedorova, L. Isaacs, *Chem. Commun.* **2015**, *51*, 1349–1352.

[54] A. Seco, A. M. Diniz, J. Sarrato, H. Mourão, H. Cruz, A. J. Parola, N. Basílio, *Pure Appl. Chem.* **2020**, *92*, 301–313.

[55] P. Ferreira, B. Ventura, A. Barbieri, J. P. Da Silva, C. A. T. Laia, A. J. Parola, N. Basílio, *Chem. Eur. J.* **2019**, *25*, 3477–3482.

[56] P. Remón, D. González, S. Li, N. Basílio, J. Andréasson, U. Pischel, *Chem. Commun.* **2019**, *55*, 4335–4338.

[57] F. Pina, M. J. Melo, C. A. T. Laia, A. J. Parola, J. C. Lima, *Chem. Soc. Rev.* **2012**, *41*, 869–908.

[58] F. Pina, M. J. Melo, M. Maestri, R. Ballardini, V. Balzani, *J. Am. Chem. Soc.* **1997**, *119*, 5556–5561.

[59] F. Pina, A. Roque, M. J. Melo, M. Maestri, L. Belladelli, V. Balzani, *Chem. -Eur. J.* **1998**, *4*, 1184–1191.

[60] F. Pina, M. Maestri, V. Balzani, *Chem. Commun.* **1999**, 107–114.

[61] F. Pina, M. J. Melo, M. Maestri, P. Passaniti, V. Balzani, *J. Am. Chem. Soc.* **2000**, *122*, 4496–4498.

[62] S. Gago, N. Basílio, A. J. Moro, F. Pina, *Chem. Commun.* **2015**, *51*, 7349–7351.

[63] A. M. Diniz, N. Basílio, H. Cruz, F. Pina, A. J. Parola, *Faraday Discuss.* **2015**, *185*, 361–379.

[64] N. Basílio, V. Petrov, F. Pina, *ChemPlusChem* **2015**, *80*, 1779–1785.

[65] B. Khungar, M. S. Rao, K. Pericherla, P. Nehra, N. Jain, J. Panwar, A. Kumar, *Comptes Rendus Chim.* **2012**, *15*, 669–674.

[66] G. Ercolani, *J. Am. Chem. Soc.* **2003**, *125*, 16097–16103.

[67] I. W. Wyman, D. H. Macartney, *Org. Biomol. Chem.* **2009**, *7*, 4045–4051.

[68] I. Neira, M. D. García, C. Peinador, A. E. Kaifer, *J. Org. Chem.* **2019**, *84*, 2325–2329.

[69] M. A. Romero, R. J. Fernandes, A. J. Moro, N. Basílio, U. Pischel, *Chem. Commun.* **2018**, *54*, 13335–13338.

[70] B. Soep, A. Kellmann, M. Martin, L. Lindqvist, *Chem. Phys. Lett.* **1972**, *13*, 241–244.

[71] M. Montalti, A. Credi, L. Prodi, M. T. Gandolfi, *Handbook of Photochemistry*, CRC Press, **2006**.

Table of Contents

A linear double pyridinium-terminated thread comprising a central *trans*-chalcone moiety forms pseudorotaxanes with cucurbit[7]uril (CB7), in water. Irradiation of the chalcone under slightly acidic conditions triggers the formation of the fluorescent cationic flavylium form with displacement of the CB7 ring along the thread, defining a pH-dependent photoswitch for ring translocation with fluorescence read-out. The system returns to the initial *trans*-chalcone state in the dark through a series of consecutive reversible reactions characteristic of flavylium-based molecular switches.